

# Collider Phenomenology of Higgsless models

Alexander Belyaev<sup>1 ab</sup>

School of Physics and Astronomy, University of Southampton, Southampton, SO17 1BJ, U.K.

**Abstract.** We study the LHC signatures of new gauge bosons in the minimal deconstruction Higgsless model (MHLM). We analyze the  $W'$  signals of  $pp \rightarrow W' \rightarrow WZ$  and  $pp \rightarrow W'jj \rightarrow WZjj$  processes at the LHC, including the complete signal and background calculation in the gauge invariant model and have demonstrated the LHC potential to cover the whole parameter space of the MHLM model.

**PACS.** 12.60.Cn Extensions of electroweak gauge sector – 12.15.Ji Applications of electroweak models to specific processes

## 1 Introduction

Disentangling the nature of electroweak symmetry breaking (EWSB) is one of the important challenges of particle physics today and upcoming CERN Large Hadron Collider (LHC), in particular. Among several appealing theories of EWSB, Higgsless models are especially promising. In particular, those models predict new heavy gauge bosons serving as a key for EWSB and delaying unitarity violation of longitudinal weak boson scattering [2,3] without invoking a fundamental Higgs scalar. Dimensional deconstruction formulation of the Higgsless theories is shown to provide their most general *gauge-invariant* formulation [3,4] under arbitrary geometry of the continuum fifth dimension (5d) or its 4d discretization with only a few lattice sites [5,6].

The Minimal Higgsless Model (MHLM) consists of just 3 lattice sites (“The Three Site Model”) [6] and predicts just two extra  $W'$  and  $Z'$  bosons which mass  $\gtrsim 400$  GeV is consistent with all the precision data [6]. MHLM is gauge invariant via spontaneous symmetry breaking and predicts just one pair of nearly degenerate new ( $W'$ ,  $Z'$ ) bosons, unlike any 5d Higgsless models with a tower of Kaluza-Klein gauge-states. This model contains all the essential ingredients of Higgsless theories being the simplest realistic Higgsless model with distinct collider signatures. In this study we investigate phenomenology of MHLM signals at the LHC including the complete signal and background calculation demonstrate demonstrated the LHC potential to cover the whole parameter space of the MHLM model.

## 2 MHLM model

The MHLM [6] is defined as a chain moose with 3 lattice sites, under the 5-dimensional  $SU(2) \times SU(2) \times U(1)$  gauge theory with electroweak symmetry breaking encoded in the boundary conditions of the gauge fields. Gauge and Goldstone sectors of MHLM have 5 parameters in total – 3 gauge couplings ( $g_0, g_1, g_2$ ) and 2 Goldstone decay constants ( $f_1, f_2$ ), satisfying two conditions due to its symmetry breaking structure,

$$\frac{1}{g_0^2} + \frac{1}{g_1^2} + \frac{1}{g_2^2} = \frac{1}{e^2}, \quad \frac{1}{f_1^2} + \frac{1}{f_2^2} = \frac{1}{v^2}. \quad (1)$$

For the optimal delay of unitarity violation we choose equal decay constant  $f_1 = f_2 = \sqrt{2}v$  where  $v = (\sqrt{2}G_F)^{-1/2}$  as fixed by the Fermi constant. Choice of  $M_W$  and  $M_{W'}$  as inputs allows to determine ( $g_0, g_1, g_2$ ) gauge couplings. The MHLM exhibits a delay of unitarity violation for weak boson scattering  $V_L^a V_L^b \rightarrow V_L^c V_L^d$  ( $V = W, Z$ ) and for  $M_{W'} \lesssim 1$  TeV, each elastic  $V_L V_L$  scattering remains unitary over the main energy range of the LHC.

The fermion sector contains SM-like chiral fermions: left-handed doublets  $\psi_{0L}$  under  $SU(2)_0$  and right-handed weak singlets  $\psi_{2R}$ . For each flavor of  $\psi_{0L}$ , there is a heavy vector-fermion doublet  $\Psi_1$  under  $SU(2)_1$ . The mass matrix for  $\{\psi, \Psi\}$  is [6]

$$M_F = \begin{pmatrix} m & 0 \\ M & m' \end{pmatrix} \equiv M \begin{pmatrix} \epsilon_L & 0 \\ 1 & \epsilon_R \end{pmatrix}. \quad (2)$$

The mass-diagonalization of  $M_F$  yields a nearly massless SM-like light fermion  $F_0$  and a heavy new fermion  $F_1$  of mass  $M_{F_1} = M\sqrt{1 + \epsilon_L^2}$ . The light SM fermions acquire small masses proportional to  $\epsilon_R$ . For the present high energy scattering analysis we only need to consider light SM fermions relevant to the proton structure functions at the LHC, which can be treated as

<sup>a</sup> Email: a.belyaev@soton.ac.uk

<sup>b</sup> the study has been done in collaboration with Hong-Jian He, Yu-Ping Kuang, Yong-Hui Qi, Bin Zhang, R. Sekhar Chivukula, Neil D. Christensen, Elizabeth H. Simmons and Alexander Pukhov [1]

massless to good accuracy. So we will set  $\epsilon_R \simeq 0$ , implying that  $\psi_{2R}$  and  $\Psi_{1R}$  do not mix.

One should stress that fermion sector plays a crucial role in the MHLM. First of all, fermion gauge couplings in the MHLM [6] are the key to ensure an exact gauge-invariance in our collider study contrary to previous studies [7]. Secondly, the fermion sector is the key which provide consistency of MHLM with precision electroweak data. The proper adjustment of amount of delocalization of fermions to amount of delocalization of gauge bosons fixes  $\epsilon_L$  via the ideal fermion delocalization [8] (IDDL) condition and leads to vanishing  $W'$ -SM fermion couplings and thus zero electroweak precision corrections at tree-level [6, 8].

One should notice that the mass of the heavy fermions is strongly bounded from below to be  $M_{F_1} > 1.8 \text{ TeV}$  [6]. Therefore the essential phenomenology of MHLM at the LHC is related to signals from new gauge bosons  $W'$  and  $Z'$  which can be as light as  $\sim 400 \text{ GeV}$ . To simplify the analysis we consistently decouple the heavy fermion by taking the limit  $(M, m) \rightarrow \infty$  while keeping the ratio  $\epsilon_L \equiv m/M$  finite. This finite ratio  $\epsilon_L$  will be fixed via IDDL [8].

We have implemented MHLM model into CalcHEP package [9] using LanHEP program [10] for automatic Feynman rules generation. This implementation has been consistently cross-checked in t'Hooft Feynman and Unitary gauges and publicly available at <http://hep.pa.msu.edu/belyaev/public/3-site/>.

### 3 Phenomenology of MHLM

As discussed above, in MHLM the couplings of new heavy bosons to SM fermions are highly suppressed to satisfy precision EW data while the couplings of new heavy bosons to SM gauge bosons are non-vanishing to provide the delay of unitarity for  $V_L^a V_L^b \rightarrow V_L^c V_L^d$  amplitudes.

These two essential features define the phenomenology of not only MHLM but the whole class of the Higgsless extradimensional models (HLED) whose phenomenology will be dominated by the first KK-mode.

In MHLM, the decay width of  $W'$  or  $Z'$  are defined by their decays to  $WZ$  or  $WW$  pairs, respectively

$$\Gamma_{V' \rightarrow WW(WZ)} = \frac{\alpha M_{V'}}{48s_Z^2 x^2} [1 + O(x^2)] \quad (3)$$

where  $\alpha = e^2/4\pi$  and  $x \equiv 2M_W/M_{W'}$ . For  $M_{W'} = (0.5 - 1) \text{ TeV}$  one has  $\Gamma_{W'} \simeq (5 - 31) \text{ GeV}$ . On the other hand, under the IDDL  $W'$  does not decay to light SM fermions while  $Z'$  decay to SM-fermions is highly suppressed

$$\Gamma_{Z' \rightarrow e^+ e^-} = \frac{5\alpha M_{V'} x^2 s_Z^2}{96c_Z^4} [1 + O(x^2)]. \quad (4)$$

Therefore, one can expect, that the most promising discovery channels would be  $Z'(W')$  production via gauge couplings with SM gauge bosons. Moreover,  $W'$  production looks more favourable since the minimal

number of neutrinos after  $W'$  leptonic decay is one ( $W' \rightarrow WZ \rightarrow 3l\nu$ ), while  $Z' \rightarrow WW \rightarrow 2l2\nu$  decay channel ends with two neutrinos disabling the reconstruction of the  $Z'$  peak.

We found that the most favorable signal processes for discovery of the MHLM at the LHC are the associated  $W'Z$  ( $pp \rightarrow W'Z \rightarrow WZZ \rightarrow 4\ell 2q$ ) production as well as  $W'$  production in  $WZ \rightarrow W$  fusion process ( $pp \rightarrow W'qq \rightarrow WZqq \rightarrow 3\ell\nu 2q$ ) representative Feynman diagrams for which are shown in Fig. 1a) and Fig. 1b), respectively. The cross sections versus  $M_{W'}$

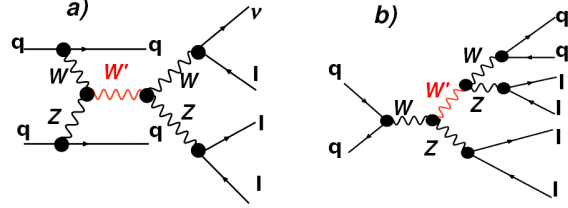


**Fig. 1.** Representative diagrams for the associated  $W'Z$  ( $pp \rightarrow W'Z \rightarrow WZZ \rightarrow 4\ell 2q$ ) production (a) as well as  $W'$  production in  $WZ \rightarrow W$  fusion process ( $pp \rightarrow W'qq \rightarrow WZqq \rightarrow 3\ell\nu 2q$ ) (b).

for  $pp \rightarrow W'Z$  and  $pp \rightarrow W'qq^{(\ell)}j$  processes including  $4\ell 2q$  and  $3\ell\nu 2q$  respective branching ratios are presented in Fig. 2. For  $pp \rightarrow W'qq^{(\ell)}j$  process the quark energy ( $E_q > 300 \text{ GeV}$ ),  $P_{Tq}$  ( $P_{Tq} > 30 \text{ GeV}$ ) and rapidity gap cuts were applied  $|\Delta\eta_{jj}| > 4$ . These cuts are essential for the background suppression as we discuss below. Hereafter we use CTEQ6L [11] parton density function and QCD scale  $Q = \sqrt{s}$  and  $Q = M_Z$  for  $pp \rightarrow W'qq^{(\ell)}$  and  $pp \rightarrow W'qq^{(\ell)}j$  processes, respectively.

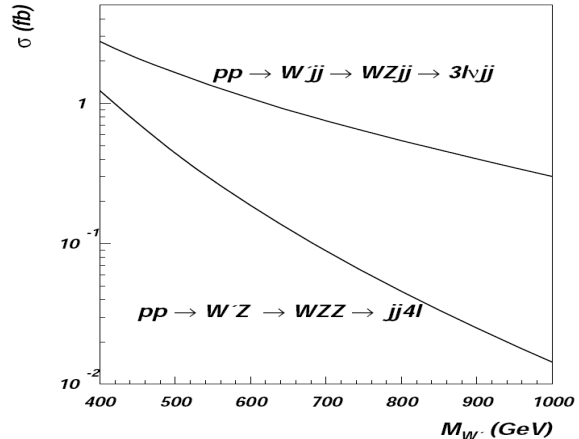


**Fig. 2.** The cross sections versus  $M_{W'}$  for  $pp \rightarrow W'Z$  and  $pp \rightarrow W'qq^{(\ell)}j$  processes including  $4\ell 2q$  and  $3\ell\nu 2q$  respective branching ratios. For  $pp \rightarrow W'qq^{(\ell)}$  process  $E_q > 300 \text{ GeV}$ ,  $P_{Tq} > 30 \text{ GeV}$  and  $|\Delta\eta_{jj}| > 4$  cuts were applied.

As we have mentioned above, we propose to analyze the  $pp \rightarrow W'Z \rightarrow WZZ$  process via leptonic decays of the two  $Z$  bosons and hadronic decays of  $W$  providing a clean signature of 4-leptons plus 2-jets,  $jj 4\ell$  ( $\ell = e, \mu$ ). The backgrounds include: (a)

the irreducible SM production of  $pp \rightarrow WZZ \rightarrow jj4\ell$ , (b) the reducible background of the SM production,  $pp \rightarrow ZZZ \rightarrow jj4\ell$ , with one  $Z \rightarrow jj$  (mis-identified as  $W$  due to finite experimental di-jet mass resolution) and (c) the SM process  $pp \rightarrow jj4\ell$  other than (a) and (b), which also includes the  $jj4\ell$  backgrounds with  $jj = qg, gg$ .

To suppress backgrounds we impose the cuts,

$$M_{jj} = 80 \pm 15 \text{ GeV}, \quad \Delta R(jj) < 1.5, \quad \sum_Z p_T(Z) + \sum_j p_T(j) = \pm 15 \text{ GeV}. \quad (5)$$

The first cut selects di-jets arising from on-shell  $W$  decay to be within the experimental resolution [12]; the second cut requires the dijet separation of the signal; and the third cut uses the conservation of transverse momentum in the signal to suppress the background. Furthermore, we impose the following electron and jet ID/acceptance cuts

$$p_{T\ell} > 10 \text{ GeV}, \quad |\eta_\ell| < 2.5, \quad p_{Tj} > 15 \text{ GeV}, \quad |\eta_j| < 4.5. \quad (6)$$

In Fig. 3 we present the  $M_{Zjj}$  event distributions for the signal and background under these cuts for an integrated luminosity of  $100 \text{ fb}^{-1}$ . We depict the signal by a dashed curve, the backgrounds (c) with  $jj = gg, qg$  by dashed and dashed-double-dotted curves, respectively, and the total background (a)+(b)+(c) by a solid curve. The backgrounds (a) and (b) are so small that they are not visible in Fig. 3. Finally we have chosen  $M_{Zjj} = M_{W'} \pm 0.04 M_{W'}$  mass window cut to estimate signal significance and LHC reach. In this mass window we have summed contributions from two  $Z$  bosons for signal and background. The gauge-invariance of this calculation is verified by comparing the signal distributions in unitary and 't Hooft-Feynman gauges; as shown in Fig. 3 by red-dashed and blue-dotted curves, they perfectly coincide. From the calculated number of

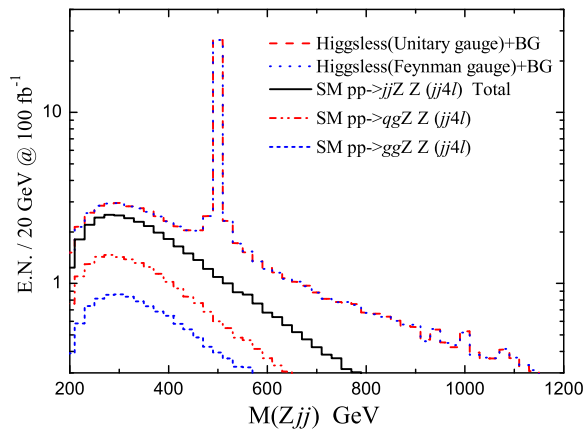


**Fig. 3.** Signal and background events in the process  $pp \rightarrow W'^{(*)}Z \rightarrow WZZ \rightarrow jj \ell^+ \ell^- \ell^+ \ell^-$  for an integrated luminosity of  $100 \text{ fb}^{-1}$ .

signal and background events, we derive the statistical significance from the Poisson probability in the conventional way. The integrated luminosity required for

detecting the  $W'$  in this channel will be summarized in Fig. 5.

Next, we analyze the LHC potential to discover  $W'$ -boson in the  $pp \rightarrow WZqq'$  process, where the signal is given by the  $W'$  contribution to  $WZ \rightarrow WZ$  scattering subprocess. We perform a complete analysis of  $pp \rightarrow WZjj$ , and choose the pure leptonic decay modes of  $WZ$  with 3 leptons plus missing- $E_T$  [13, 14]. We carry out a full tree-level calculation including both signal and background together.

To effectively suppress  $qq \rightarrow WZ$  and  $pp \rightarrow WZjj$  ( $jj = qg, gg$ ) QCD backgrounds we apply the following jets rapidity gap cut and large jet energy cut

$$|\Delta\eta_{jj}| > 4, \quad E_j > 300 \text{ GeV} \quad (7)$$

in addition to acceptance cuts given by

$$p_{Tj} > 30 \text{ GeV}, \quad |\eta_j| < 4.5, \quad p_{T\ell} > 10 \text{ GeV}, \quad |\eta_\ell| < 2.5 \quad (8)$$

where  $E_j$  and  $p_{Tj(l)}$  are transverse energy and momentum of final-state jet(lepton),  $\eta_{j(l)}$  is the jet(lepton) rapidity, and  $|\Delta\eta_{jj}|$  is the difference between the rapidities of the two forward jets. For computing the SM EW backgrounds, we need to specify the reference value of the SM Higgs mass  $M_H$ . Because the SM Higgs scalar only contributes to the  $t$ -channel in  $pp \rightarrow qq'WZ$ , we find that varying the Higgs mass in its full range  $M_H = 115 \text{ GeV} - 1 \text{ TeV}$  has little effect on the SM background curve. Hence we can simply set  $M_H = 115 \text{ GeV}$  in our plots without losing generality.

Using cuts (7)-(8) we have computed the  $WZ$  invariant mass ( $M_{WZ}$ ) distribution in both unitary gauge and 't Hooft-Feynman gauge and have revealed an extremely precise and large cancellation between the fusion and non-fusion contributions for  $pp \rightarrow WZqq'$  process, as required by the exact gauge-invariance. These cancellations cannot be inferred without a truly gauge-invariant model, contrary to the approach of imposing only a naive 5d sum rule [7]. Traditional analyses [13] of gauge-boson fusion in a strongly-interacting symmetry breaking sector have relied on using separate calculations of the signal and background while in our case in the correct gauge-invariant implementation of MHLM we can perform direct calculation of  $qq \rightarrow WZqq'$  process for signal and background together.

Since there is just one neutrino in  $3\ell\nu$  signature, we can use transverse mass variable,  $M_T^2(WZ) = [\sqrt{M^2(\ell\ell\ell) + p_T^2(\ell\ell\ell)} + |p_T^{\text{miss}}|^2] - [p_T(\ell\ell\ell) + p_T^{\text{miss}}]^2$  [13] for the effective signal over the background rejection. In Fig. 4 we present  $M_T^2(WZ)$  distributions for  $M_{Z'} = 500, 700, 900 \text{ GeV}$  exhibiting clear Jacobian peaks. We compute signal significance for the  $0.85M_{W'} < M_T < 1.05M_{W'}$  window and obtain the required integrated luminosities for  $3\sigma$  and  $5\sigma$  detections of the  $W'$  boson presented in Fig. 5.

## 4 Summary

We present the first study on LHC potential to observe signatures predicted by Minimal Higgsless Model

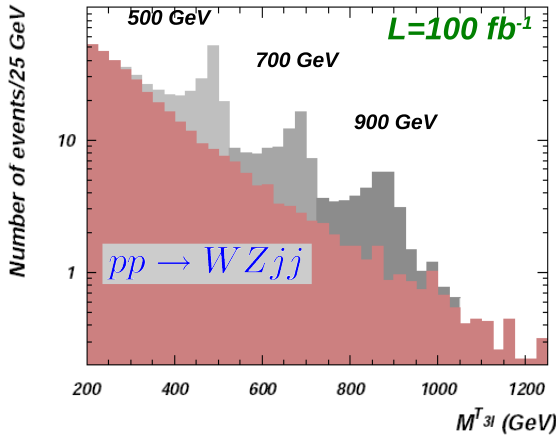


**Fig. 4.** Numbers of signal and background events versus the transverse mass  $M_T(WZ)$  after imposing the cuts (7)-(8) for an integrated luminosity of  $100 \text{ fb}^{-1}$ .

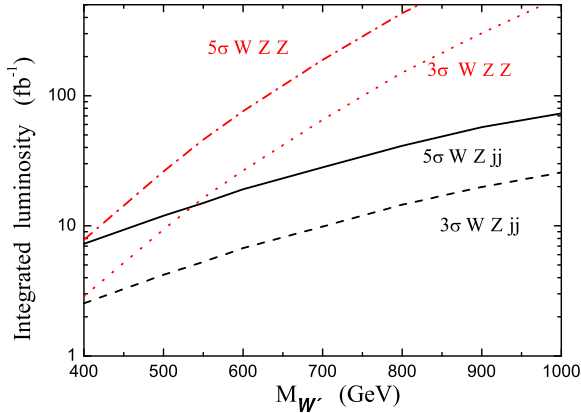


**Fig. 5.** Integrated luminosities required for  $3\sigma$  and  $5\sigma$  detection of  $W'$  signals as a function of  $M_{W'}$ . The dotted and dashed-dotted curves are for the  $WZZ$  channel, while the dashed and solid curves are for the  $WZjj$  channel.

(MHLM) [6]. We have calculated the complete gauge invariant signals and backgrounds for two promising processes,  $pp \rightarrow WZZ \rightarrow jj4\ell$  and  $pp \rightarrow WZjj \rightarrow \nu 3\ell jj$ . In this analysis, we only take account of the statistical error. We have checked that typical electromagnetic ( $0.1/\sqrt{E(\text{GeV})}$ ) and hadronic ( $0.5/\sqrt{E(\text{GeV})}$ ) detector energy resolution [12] which we have approximated by gaussian smearing, has a very small effect on the presented distributions (Fig.3,4) and final results (Fig.5). Other issues related to the details of detectors, such as the systematic error, detection efficiency, etc, are beyond this study. Both  $WZZ$  and  $WZqq'$  channels have clean leptons signatures and reconstructable  $W'$  mass. With the proposed cuts we can effectively suppress all SM backgrounds. We would like to stress that the calculation in the context of an exactly gauge-invariant Higgsless model (such as the MHLM [6]), is vital for analyzing the  $pp \rightarrow WZjj$  process consistently. One should also stress the complementarity of  $WZZ$  and  $WZqq'$  channels. The first one provide clean resonance peak and would allow the precise reconstruction of the  $W'$  mass while the second one has larger cross section and with  $100 \text{ fb}^{-1}$  integrated luminos-

ity would allow to completely cover MHLM parameter space up to unitarity limit at  $M_{W'} \simeq 1.2 \text{ TeV}$ . We summarize the  $3\sigma$  and  $5\sigma$  detection potential of the LHC in Fig. 5 where the required integrated luminosities are shown. For example, for  $M_{W'} = 500$  (400) GeV, the  $5\sigma$  discovery of  $W'$  requires an integrated luminosity of  $26$  ( $7.8$ )  $\text{fb}^{-1}$  for  $pp \rightarrow WZZ \rightarrow jj4\ell$ , and  $12$  ( $7$ )  $\text{fb}^{-1}$  for  $pp \rightarrow WZjj \rightarrow \nu 3\ell jj$ . These are within the reach of the first few years run at the LHC. The evidence for both signals from the  $W'$  boson, as well as the *absence* of a Higgs-like signal in  $pp \rightarrow ZZqq \rightarrow 4\ell qq$ , will be strong evidence for Higgsless electroweak symmetry breaking.

To conclude, for the first time we have consistently studied MHLM model which is very well motivated and has several appealing features: it is simple but generic, since the phenomenology of any Higgsless extradimensional model is dominated by the first KK-mode; the perturbatively calculable MHLM could shed a light on its conjectured dual strongly interacting theory; MHLM consistently implements the first KK-mode in a gauge-invariant way; MHLM satisfies precision EW measurements, suggests a very distinctive phenomenology while its parameter space, as we have shown, is fully testable at the LHC.

**Acknowledgments:** A. B. thanks SUSY 2007 organizers for warm hospitality.

## References

1. H. J. He *et al.*, arXiv:0708.2588 [hep-ph].
2. R. S. Chivukula, D. A. Dicus, H.-J. He, Phys. Lett. B **525**, 175 (2002); R. S. Chivukula, H.-J. He, Phys. Lett. B **532**, 121 (2002). R. S. Chivukula, D. A. Dicus, H.-J. He, S. Nandi, Phys. Lett. B **562**, 109 (2003).
3. H.-J. He, Int. J. Mod. Phys. A **20**, 3362 (2005).
4. R. S. Chivukula, E. H. Simmons, H.-J. He, M. Kurachi, M. Tanabashi, Phys. Rev. D **70**, 075008 (2004); Phys. Rev. D **71**, 035007 (2005).
5. R. S. Chivukula, E. H. Simmons, H.-J. He, M. Kurachi, M. Tanabashi, Phys. Rev. D **71**, 115001 (2005).
6. R. S. Chivukula, B. Coleppa, S. Di Chiara, E. H. Simmons, H.-J. He, M. Kurachi, M. Tanabashi, Phys. Rev. D **74**, 075011 (2006).
7. A. Birkedal, K. Matchev and M. Perelstein, Phys. Rev. Lett. **94**, 191803 (2005).
8. R. S. Chivukula, E. H. Simmons, H.-J. He, M. Kurachi, M. Tanabashi, Phys. Rev. D **72**, 015008 (2005); D **72**, 095013 (2005).
9. A. Pukhov, arXiv:hep-ph/0412191.
10. A. V. Semenov, arXiv:hep-ph/0208011.
11. J. Pumplin, D. R. Stump, J. Huston, H. L. Lai, P. Nadolsky and W. K. Tung, JHEP **0207**, 012 (2002) [arXiv:hep-ph/0201195].
12. ATLAS Physics TDR, *Detector and Physics Performance – Technical Design Reports*, CERN/LHCC/99-15, vol. 1.
13. J. Bagger, *et al.*, Phys. Rev. D **52**, 3878 (1995).
14. H.-J. He, Y.-P. Kuang, C.-P. Yuan, B. Zhang, Phys. Lett. B **554**, 64 (2003); B. Zhang, Y.-P. Kuang, H.-J. He, C.-P. Yuan, Phys. Rev. D **67**, 114024 (2003).